JOURNAL OF MAGNETIC RESONANCE, Series A **119,** 134–138 (1996)
ARTICLE NO. 0063

Increased HMBC Sensitivity for Correlating Poorly Resolved Proton Multiplets to Carbon-13 Using Selective or Semi-selective Pulses

AD BAX,* KATHLEEN A. FARLEY,† AND GREGORY S. WALKER†

*Laboratory of Chemical Physics, National Institutes of Diabetes and Digestive and Kidney Diseases, National Institutes of Health, Bethesda, Maryland 20892-0520; and †Analytical Research and Specifications Development, Pharmacia & Upjohn Inc., Kalamazoo, Michigan 49001-0199

Received November 6, 1995

Correlations based on scalar coupling between protons and carbons separated by two or three chemical bonds are very useful for structure determination of organic molecules. In particular, the heteronuclear multiple-bond correlation experiment (HMBC) has become widely used for this purpose (*1*). This experiment enjoys the increased sensitivity resulting from detection of the NMR-sensitive ^{1}H spin, and, in contrast to most of the ^{13}C-detected analogs, long-range correlation intensities are not affected by the size of the one-bond J_{CH} couplings. The HMBC experiment requires a relatively long delay for obtaining ^{1}H magnetization in antiphase with its long-range coupled ^{13}C, prior to generation of multiple-quantum coherence. Similarly, after the evolution period, ^{1}H magnetization becomes observable only after it is rephased with respect to its long-range ^{13}C coupling partner. During these lengthy (30–100 ms) dephasing and rephasing periods, the ^{1}H magnetization is also subject to homonuclear ^{1}H–^{1}H J modulation, and the detected ^{1}H multiplet generally will have significant antiphase contributions resulting from the homonuclear multiplet structure. Particularly for protons with an unresolved or poorly resolved ^{1}H–^{1}H multiplet structure, this tends to result in low sensitivity for its long-range correlations to ^{13}C. Below, we describe how the sensitivity of the HMBC experiment can be increased, sometimes by as much as an order of magnitude, by using semi-selective pulses which suppress homonuclear ^{1}H–^{1}H J modulation.

Selective and semi-selective pulses previously have been widely used on the ^{13}C channel of the HMBC pulse sequence (*2–6*). The purpose of using frequency-selective pulses in these experiments was to reduce the spectral window needed in the F_1 (^{13}C) dimension of the 2D spectrum, thereby permitting the spectrum to be recorded at higher resolution for a given number of increments. Note, however, that using selective pulses in this application does not increase the sensitivity of the experiment: The increased number of scans per t_1 increment is offset by the lower number of t_1 increments if the total measuring time is kept constant. On the other hand, the purpose of using selective or semi-selective ^{1}H pulses in the HMBC experiment is to increase its sensitivity, in much the same way as the use of selective ^{1}H pulses in the refocused INEPT (*7, 8*) experiment can be used to transfer magnetization more effectively through long-range ^{1}H–^{13}C couplings (*9, 10*).

Figure 1 shows three different implementations of the ^{1}H-selective HMBC experiment. Selection of the appropriate scheme depends on the particular application. Several of the experimental details will be discussed later, but first we briefly discuss when to use which pulse sequence. The scheme of Fig. 1A is the simplest and is identical to the regular HMBC pulse scheme, except that the ^{1}H RF power is attenuated and the carrier position is selected such that the proton of interest, but not the protons J-coupled to the proton of interest, experiences the 180° pulse. If the ^{1}H of interest is sufficiently separate from its coupling partners in the ^{1}H spectrum, such that the duration of the 180° ^{1}H pulse does not need to exceed 2–3 ms for achieving the desired selectivity, the scheme of Fig. 1A can be used. If the duration of the 180° pulse needs to be longer than a few milliseconds, the scheme of Fig. 1B is preferred. In contrast to the regular nonselective HMBC experiment, the schemes of Figs. 1A and 1B do not remove the heteronuclear J coupling evolution of the carbon in the t_1 dimension. In practice, this will limit the spectral resolution that can be obtained in the ^{13}C dimension. The scheme of Fig. 1C solves this problem and yields a spectrum with full heteronuclear decoupling. In contrast to the schemes of Figs. 1A and B, this sequence permits the spectrum to be recorded in the phase-sensitive mode, further increasing the obtainable spectral resolution. Examples of all three schemes will be shown for the cyclic decapeptide gramicidin S.

As mentioned above, the scheme of Fig. 1A is essentially identical to the original HMBC experiment, except for the use of pulsed field gradients to achieve coherence-pathway selection, and the use of selective ^{1}H pulses to ensure refocusing of the homonuclear couplings at time $t_1 + \Delta$ after the 180° ^{1}H pulse. The RF field strength used for the 90° ^{1}H pulse is arbitrary and may, for convenience, be set to the same value as that used for the 180° ^{1}H pulse. The 180° ^{1}H pulse may be either shaped or rectangular, and its frequency

1064-1858/96 $18.00

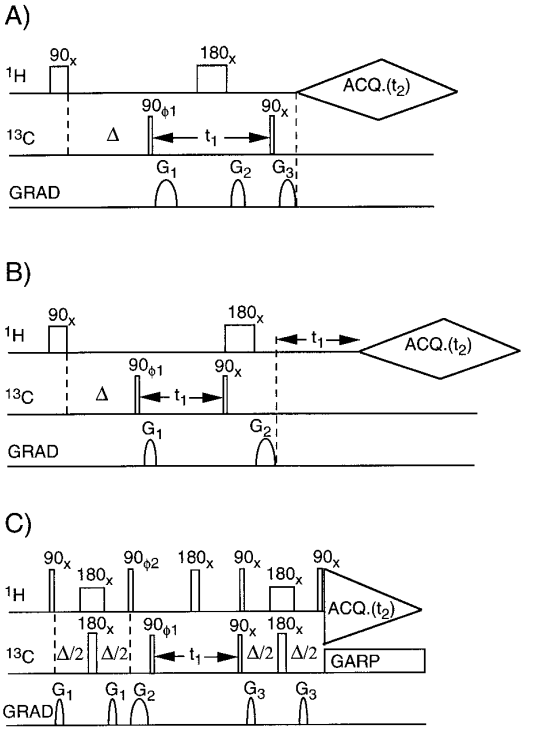

FIG. 1. Selective HMBC pulse sequences. (A) Regular HMBC scheme, containing a frequency-selective ^{1}H pulse to invert the proton of interest, but not its homonuclear coupling partners. The power level for the 90° ^{1}H pulse is arbitrary. Pulsed field gradients (sine-bell shaped, 25 G/cm at center) are used for coherence selection: $G_{1,2,3}$ = 500, 300, 402 μs. Phase cycling: $\phi_1 = x, -x$; Acq. $= x, -x$. The duration of Δ is optimized for long-range correlation, $\Delta \approx (2\ ^{lr}J_{CH})^{-1}$, and can be somewhat longer than in the regular nonselective HMBC experiment. For correlation to protonated carbons, X, sensitivity considerations suggest incrementing the t_1 duration (which includes G_1, G_2, and the 180° ^{1}H pulse) from $0.6/^1J_{XH}$ to $1.4/^1J_{XH}$. For correlation to nonprotonated ^{13}C nuclei, this restriction on the t_1 acquisition time does not apply. (B) Modified selective HMBC scheme for correlating a selected proton to protonated ^{13}C nuclei, used when the duration of the selective ^{1}H 180° pulse is longer than a few milliseconds. Pulsed field gradients are used for coherence selection: $G_{1,2}$ = 799, 1000 μs. Phase cycling: $\phi_1 = x, -x$; Acq. $= x, -x$. For correlation to protonated carbons, X, sensitivity considerations suggest incrementing the t_1 duration (which includes G_1) from $0.6/^1J_{XH}$ to $1.4/^1J_{XH}$. Spectra recorded with both schemes (A) and (B) require a t_2 acquisition time of about 2Δ. Processing: Absolute value mode, using sine bell apodization in t_2 and a ~20° shifted sine bell in the t_1 dimension. (C) Heteronuclear multibond correlation using heteronuclear single-quantum coherence (HSQC) for generating 2D absorptive, heteronuclear-decoupled long-range correlation spectra. Pulsed field gradients are used for coherence-pathway suppression (*19*): $G_{1,2,3}$ = 0.5, 3, 0.3 ms. Phase cycling: $\phi_1 = x, x, -x, -x$; $\phi_2 = x, -x$; Acq. $= x, -x, -x, x$. For optimal suppression of t_1 noise, the phase of the low-power 180° pulse must be carefully adjusted to correspond to the same value as for the high-power 90° pulses (see text). Quadrature in the t_1 dimension is obtained in the regular manner by incrementing ϕ_1 in the States (*20*), States–TPPI (*21*), or TPPI (*22*) manner. Code for the pulse sequence on a Bruker AMX spectrometer has been deposited at the BioMagResBank, Madison, WI (http://www.bmrb.wisc.edu).

selectivity is not particularly critical. If the proton resonating nearest to the selected proton is separated by W hertz in the ^{1}H spectrum, a rectangular 180° ^{1}H pulse with an RF field strength of $W/\sqrt{3}$ hertz generally will yield reasonable results. The duration of the pulsed field gradients is set such that coherence-pathway selection is achieved effectively, resulting in minimal t_1 noise. On the spectrometer used in the present study, this requires durations of 500, 300, and 402 μs for gradients G_1, G_2, and G_3, which were sine-bell shaped, with a strength of 25 G/cm at their midpoint. The pulsed field gradients were sine-bell shaped because that is the simplest way to program pulsed field gradients with the homebuilt gradient hardware used, and rectangular gradients should yield comparable results.

If the $90^\circ_{\phi 1}$ pulse in Fig. 1A generates heteronuclear multiple-quantum coherence between a proton, A, and a carbon, X, heteronuclear scalar couplings between X and protons other than A are not decoupled during t_1. Therefore, if X is a protonated carbon, the multiple-quantum coherence will be modulated by $^1J_{XH}$ in the t_1 dimension, resulting in a loss in sensitivity and resolution. If X has n directly attached protons, the envelope of the t_1 time-domain signal is modulated by $\cos^n(\pi J_{XH} t_1)$, where the t_1 duration includes the time needed for gradient pulses G_1 and G_2 and the time needed for the 180° ^{1}H pulse. By restricting the sampling in the t_1 dimension to $0.6/^1J_{XH} < t_1 < 1.4/^1J_{XH}$, one measures that the time domain in the t_1 dimension has the shape of a sine bell to the power n, slightly truncated at both the beginning and the end. Reasonable sensitivity is then obtained by using digital filtering with a window which approximates this shape in the t_1 dimension. In analogy with the regular HMBC experiment, the full echo is acquired in the t_2 dimension by using an acquisition time of approximately 2Δ. Digital filtering with a sine bell or similarly shaped window function in the t_2 dimension will provide optimal sensitivity and resolution in the final absolute-value-mode spectrum. As pulsed field gradients are used for coherence-pathway selection (*11, 12*), the detected data are truly phase-modulated and generation of a ''mixed-mode'' spectrum (*13*), absorptive in the F_1 dimension but absolute value mode in F_2, is no longer straightforward.

If the duration of the 180° pulse needed to achieve sufficient selectivity in the scheme of Fig. 1A is more than a few milliseconds, the first t_1 increment becomes significantly longer than $0.6/^1J_{XH}$. Except for cases where one just wants to establish long-range correlations between a proton and nonprotonated ^{13}C nuclei, it becomes advantageous to use the scheme of Fig. 1B instead. In this scheme, the selective ^{1}H 180° pulse is shifted to the right of the multiple-quantum evolution period. When using $G_2 = G_1(\gamma_H + \gamma_C)/\gamma_H$, the pulse sequence selects ^{1}H– ^{13}C double-quantum coherence and, in the absence of the additional t_1 evolution period after the selective ^{1}H 180° pulse, the detected signal would be modulated by $\delta_C - \delta_H$, where δ_C and δ_H are the angular offset frequencies of the ^{1}H and ^{13}C involved, respectively. (Note that the selective ^{1}H pulse inverts the phase accumulated by

the ^{1}H during the first t_1 period.) Insertion of the second t_1 period offsets the ^{1}H chemical-shift contribution accumulated during the first t_1 evolution period, and the detected signal then becomes phase-modulated by ^{13}C chemical shift only (in the ^{1}H-coupled mode). Again, for detection of long-range correlations to protonated ^{13}C nuclei, the t_1 acquisition window is chosen to fall in the range $0.6/^1J_{XH} < t_1 < 1.4/^1J_{XH}$.

For the schemes of Figs. 1A and B, resolution in the 2D spectrum is limited by the short t_1 acquisition time, resulting from the $0.6/^1J_{XH} < t_1 < 1.4/^1J_{XH}$ requirement and by the absolute-value-mode display of the spectrum. Both limitations are removed by recording the experiment as a heteronuclear single-quantum-coherence (HSQC) correlation (*14*), optimized for the detection of long-range connectivities (Fig. 1C). The durations of the delays, Δ, needed for de- and rephasing ^{1}H magnetization relative to ^{13}C, are optimized for the size of the long-range J_{CH} coupling. Dephasing resulting from homonuclear ^{1}H–^{1}H J coupling is again suppressed by using frequency-selective 180° pulses at the midpoints of the Δ intervals. As pulsed field gradients are not used for coherence selection, particular care is needed to minimize t_1 noise resulting from the vast majority of protons not coupled to ^{13}C. This is accomplished in two stages: First, magnetization which has not dephased with respect to ^{13}C during the first Δ period remains along the ϕ_2 axis after the $90^\circ_{\phi 2}$ pulse and is effectively dephased by the G_2 ''scrambling gradient.'' Second, any longitudinal ^{1}H magnetization present at the end of the t_1 duration is returned to the z axis by an additional 90°_x ^{1}H pulse immediately prior to data acquisition. Depending on spectrometer type, the absolute phase of the low-power 180°_x pulses may differ from those of the high-power 90°_x pulses. Therefore, the phase of the low-power 180°_x pulse is carefully adjusted to minimize ^{1}H signals detected in a single-scan experiment which uses a 90°_x (nonselective ^{1}H)—$\Delta/2(G_3)$—180°_x (selective ^{1}H)—$\Delta/2(G_3)$—90°_x (nonselective ^{1}H) excitation sequence. The gradient pairs G_1 and G_3 in Fig. 1C eliminate the effects of imperfections in the inversions of the 180° (^{1}H) pulses. Use of the pulsed field gradients and the final 90°_x (^{1}H) pulse as described above attenuated t_1 noise in our experimental setup by at least 20-fold, to below the detectable level.

Experiments were conducted at 600 MHz on a Bruker AMX-600 spectrometer, equipped with a triple-resonance pulsed-field-gradient probehead, containing a self-shielded z gradient, and using a homebuilt gradient power supply. Spectra were recorded of a solution containing 17 mM of the cyclic decapeptide gramicidin S, c(Pro–Val–Orn–Leu–Phe)$_2$, dissolved in 94% DMSO-d_6, 6% H_2O.

Figure 2 compares the results obtained for the H$^\alpha$ region of the spectrum with (2A) the regular nonselective HMBC experiment, (2B) the scheme of Fig. 1A, using a selective pulse which excites the entire ^{1}H$^\alpha$ spectral region but not the ^{1}H$^\beta$ or ^{1}H^N resonances, and (2C) the selective HSQC experiment of Fig. 1C. The duration of Δ was 60 ms for each of the three experiments. All nonselective ^{1}H pulses were applied using a 25 kHz RF field, all ^{13}C pulses used a 21.5 kHz RF field, and ^{13}C decoupling used a 4.2 kHz RF field. The RF power of all selective ^{1}H pulses was adjusted to yield an RF field of 250 Hz (1 ms 90° pulse width). The absolute-value-mode spectra of Figs. 2A and B each were acquired using 170 increments with four scans per t_1 increment and a total measuring time of 13 min per experiment. Contours in both spectra are plotted at the same level relative to the thermal noise. Since ^{1}H–^{13}C dephasing occurs during the first selective ^{1}H 90° pulse in the scheme of Fig. 1A, the effective total dephasing time in this experiment is slightly ($\sim$630 μs) longer compared to using nonselective ^{1}H pulses. This results in different intensities of the nonsuppressed one-bond correlations (connected by horizontal lines in Fig. 2B) in the two spectra. The sensitivity in the selective HMBC spectrum of Fig. 2B is marginally higher (10–50%) for the correlations to Orn, Leu, and Val H$^\alpha$, about twofold higher for correlations to Pro-H$^\alpha$, and about fourfold higher for correlations to Phe H$^\alpha$. For the regular HMBC spectrum (Fig. 2A), the correlations to Phe C$^\beta$ and C$^\gamma$ fall below the detection threshold at the contour level shown, whereas they yield clearly observable correlations in the selective HMBC spectrum of Fig. 2B.

The spin state of the ^{1}H$^\beta$ protons remains unchanged in the experiment of Fig. 1A, with the ^{1}H selective pulses applied to ^{1}H$^\alpha$. As a result, the correlations to the protonated ^{13}C$^\beta$ nuclei show an ''E.COSY''-like pattern (*15*), resulting in a distinct ''tilt'' of the correlations between ^{1}H$^\alpha$ and ^{13}C$^\beta$ resonances in Fig. 2B. The correlations to protonated ^{13}C$^\gamma$ and ^{13}C$^\delta$ resonances are also broadened by unresolved $^1J_{CH}$ couplings in the F_1 dimension, but the correlations to nonprotonated carbonyls are not affected relative to the spectrum of Fig. 1A. Note, however, the apparent small shifts in resonance positions for the partially overlapping correlations between H$^\alpha$ and its intraresidue and sequential carbonyls in both the spectra of Figs. 2A and 2B (relative to Fig. 2C). This is a known artifact resulting from the absolute-value-mode display of the data.

The selective HSQC spectrum shown in Fig. 2C is purely absorptive, and resonance positions are far closer to their true chemical-shift positions. This spectrum was recorded using 256 complex t_1 increments, using eight scans per complex t_1 increment, and a total acquisition time of 40 min. The resolution in Fig. 1C is superior to what can be achieved with the HMBC schemes, but after correction for the difference in measuring times, the signal-to-noise ratio of the selective HSQC spectra is somewhat lower ($\sim$10–25%) than that obtained with the schemes of Figs. 1A and 1B.

Figure 3 compares the results obtained with the regular HMBC experiment (128 scans) with that shown in Fig. 1B,

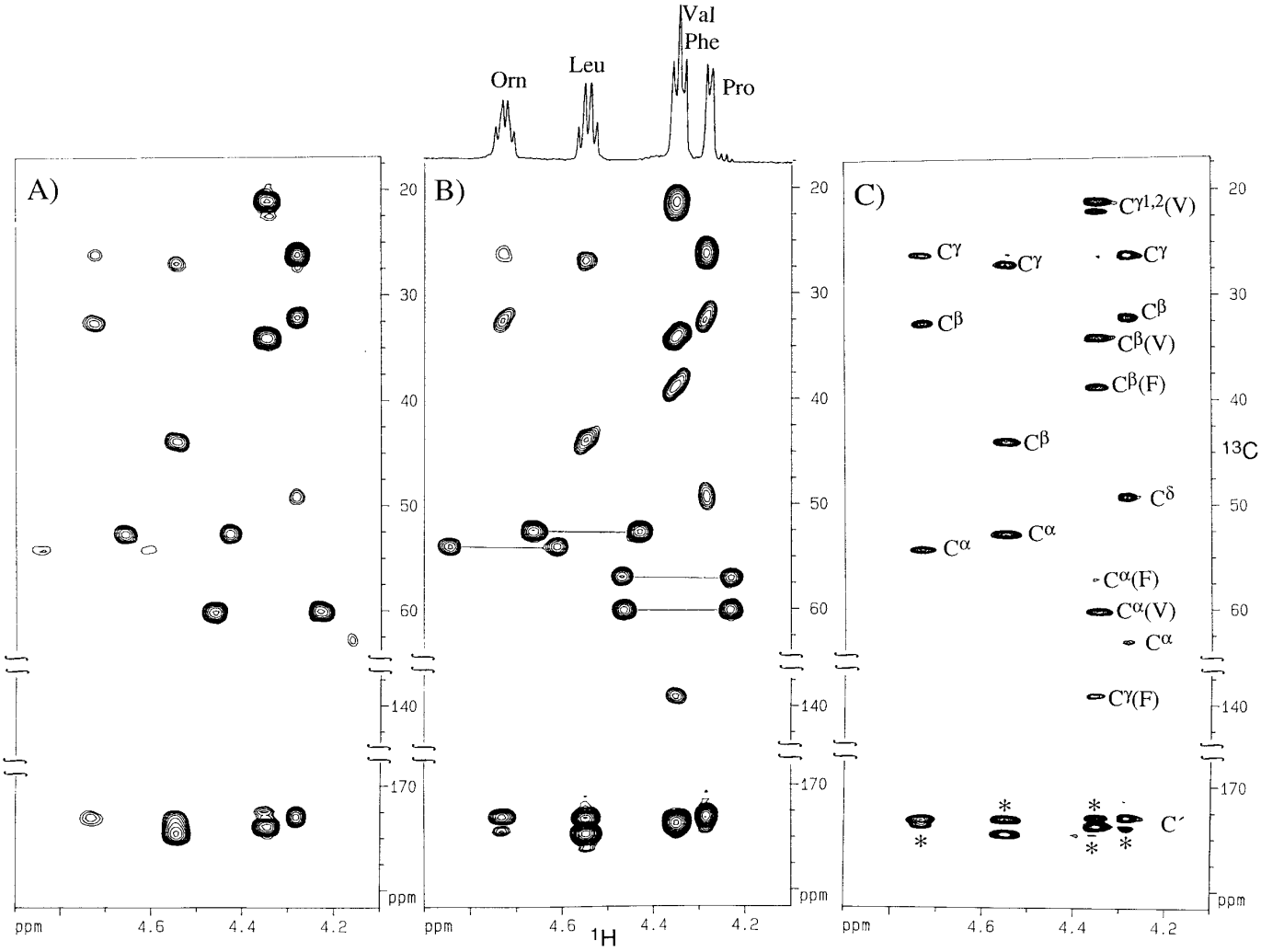

FIG. 2. $^{1}H^{\alpha}-{}^{13}C$ correlations recorded with HMBC experiments for a 17 m*M* sample of gramicidin S at 600 MHz, using heteronuclear dephasing delays, Δ, of 60 ms. Spectrum recorded (A) with the regular nonselective HMBC experiment, and (B) with the scheme of Fig. 1A, using a rectangular 2 ms 180° selective pulse and the ^{1}H carrier set to 4.45 ppm. Spectra (A) and (B) are displayed in the absolute value mode and result from 170 t_1 increments of 38 μs each (acquisition time: 13 min per spectrum). (C) Two-dimensional absorption mode $^{1}H^{\alpha}-{}^{13}C$ long-range correlation spectrum, using rectangular 2 ms 180° ^{1}H selective pulses, and 256 complex t_1 increments of 38 μs each (eight scans per complex t_1 increment, total acquisition time 40 min). Except for correlations between H^{α} of residue *i* and the carbonyl of $i-1$, marked by asterisks, all correlations are intraresidue. Correlations for the overlapping H^{α} resonances of Val (V) and Phe (F) are marked by residue type, too. All three spectra are plotted at the same contour level relative to the thermal noise.

for correlations to $H^{\beta 2}$ of the two equivalent Pro residues in the peptide. The homonuclear multiplet structure of this proton is completely unresolved (Fig. 3A), and as a consequence, the regular HMBC spectrum (Fig. 3B) yields very poor signal-to-noise, even after an 8-h experiment. In contrast, the selective HMBC scheme of Fig. 1B, using a 7.5 ms 180° ^{1}H pulse duration, yields excellent sensitivity in just four scans (total time 13 min), providing an increase in sensitivity by more than an order of magnitude.

The use of ferquency-selective ^{1}H pulses in HMBC experiments can dramatically increase the sensitivity of correlations to protons with poorly resolved homonuclear multiplet structures. As illustrated by the Val and Phe H^{α} resonances in Fig. 2, the selected ^{1}H resonance does not need to be free of overlap; it merely needs to be separated by more than about 0.1 ppm from any homonuclear coupling partner, such that its resonance can be inverted without inverting that of the coupled spins.

The use of selective ^{1}H pulses may be combined with that of frequency-selective ^{13}C pulses (*2–6*), although the F_1 resolution in the schemes of Figs. 1A and 1B will remain limited by the $^{13}C-\{^{1}H\}$ multiplet structure which frequently cannot be resolved without sacrificing sensitivity. If the experiment is needed to investigate long-range connec-

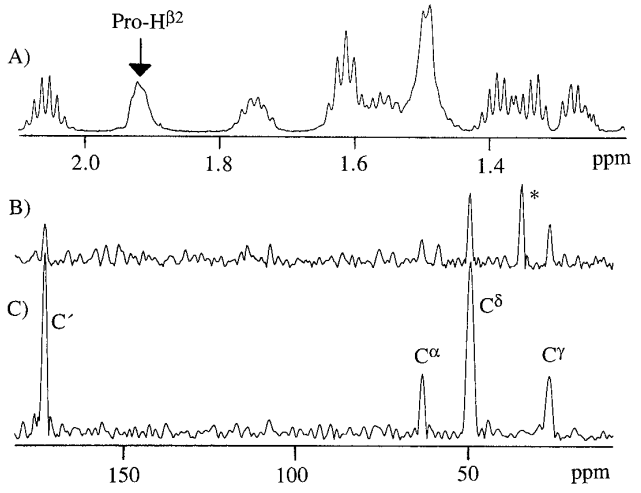

FIG. 3. (A) Small region of the 1D ^{1}H spectrum of gramicidin S, showing the unresolved multiplet of Pro-H$^{\beta 2}$. (B, C) F_1 traces taken through the HMBC spectra at the F_2 frequency of Pro-H$^{\beta 2}$. (B) Regular, nonselective HMBC, 128 scans per t_1 increment (8 h). (C) Selective HMBC, recorded with the scheme of Fig. 1B, using $\Delta = 60$ ms, and a 7.5 ms 180° ^{1}H pulse width (total acquisition time, 13 min). In (B), the resonance marked with an asterisk corresponds to the one-bond ^{1}H$^{\beta}-^{13}$C$^{\beta}$ correlation of Val.

tivity between a proton and a protonated ^{13}C, the experiment is best performed with a short t_1 acquisition time, optimized in the manner described above, and the small number of t_1 increments will remove any need to use frequency-selective 13C pulses. If very high resolution in the ^{13}C dimension is required, the scheme of Fig. 1C is preferred because it yields purely absorptive spectra and, in contrast to regular nonselective HMBC, F_1 resolution is not affected by ^{1}H$-^1$H J couplings. For quantitative measurement of ^{13}C$-^1$H long-range couplings, $^{lr}J_{CH}$, a number of selective HSQC spectra can be recorded in which the first Δ delay (prior to t_1) is systematically incremented from, for example, 50 to 250 ms. The correlation intensities then can be fitted to a $\sin(\pi\,{}^{lr}J_{CH}\Delta)\exp(-\Delta/T_{2H})$ function, where T_{2H} is the transverse-relaxation time of the proton of interest. Provided signal-to-noise is adequate, this approach provides very reliable measurements for $^{lr}J_{CH}$ (*16–18*).

REFERENCES

1. A. Bax and M. F. Summers, *J. Am. Chem. Soc.* 108, 2093 (1986).
2. W. Bermel, K. Wagner, and C. Griesinger, *J. Magn. Reson.* 83, 223 (1989).
3. H. Kessler, P. Schmieder, M. Köck, and M. Kurz, *J. Magn. Reson.* 88, 615 (1990).
4. R. C. Crouch and G. E. Martin, *J. Magn. Reson.* 92, 189 (1991).
5. H. Kessler, S. Mronga, and G. Gemmecker, *Magn. Reson. Chem.* 29, 527 (1991).
6. R. C. Crouch, T. D. Spitzer, and G. E. Martin, *Magn. Reson. Chem.* 30, 595 (1992).
7. G. A. Morris and R. Freeman, *J. Am. Chem. Soc.* 101, 760 (1979).
8. D. P. Burum and R. R. Ernst, *J. Magn. Reson.* 39, 163 (1980).
9. A. Bax, C. H. Niu, and D. Live, *J. Am. Chem. Soc.* 106, 1150 (1984).
10. A. Bax, *J. Magn. Reson.* 57, 314 (1984).
11. R. E. Hurd and B. K. John, *J. Magn. Reson.* 91, 648 (1991).
12. W. Wilker, D, Leibfritz, R. Kerssebaum, and W. Bermel, *Magn. Reson. Chem.* 31, 287 (1993).
13. A. Bax and D. Marion, *J. Magn. Reson.* 78, 186 (1988).
14. G. Bodenhausen and D. J. Ruben, *Chem. Phys. Lett.* 69, 185 (1980).
15. C. Griesinger, O. W. Sørenson, and R. R. Ernst, *J. Chem. Phys.* 85, 6837 (1986).
16. D. Neri, G. Otting, and K. Wüthrich, *J. Am. Chem. Soc.* 112, 3663 (1990).
17. M. Billeter, D. Neri, G. Otting, Y. Q. Qian, and K. Wüthrich, *J. Biomol. NMR* 2, 257 (1992).
18. H. Kuboniwa, S. Grzesiek, F. Delaglio, and A. Bax, *J. Biomol. NMR* 4, 871 (1994).
19. A. Bax and S. S. Pochapsky, *J. Magn. Reson.* 99, 638 (1992).
20. D. J. States, R. A. Haberkorn, and D. J. Ruben, *J. Magn. Reson.* 48, 286 (1982).
21. D. Marion, M. Ikura, R. Tschudin, and A. Bax, *J. Magn. Reson.* 85, 393 (1989).
22. D. Marion and K. Wüthrich, *Biochem. Biophys. Res. Commun.* 113, 967 (1983).